

BER Performance of IM/DD FSO System with OOK using APD Receiver

Milica I. PETKOVIĆ, Goran T. ĐORĐEVIĆ, Dejan N. MILIĆ

University of Niš, Faculty of Electronic Engineering, Dept. of Telecommunications,
Aleksandra Medvedeva 14, 18000 Niš, Serbia

milicapetkovic86@gmail.com, goran@elfak.ni.ac.rs, dejan.milic@elfak.ni.ac.rs

Abstract. *In this paper, the performance of intensity-modulated with direct detection (IM/DD) free space optical (FSO) system using the on-off keying (OOK) and avalanche photodiode (APD) receiver is observed. The gamma-gamma model is used to describe the effect of atmospheric turbulence since it provides good agreement in the wide range of atmospheric conditions. In addition, the same FSO system with equal gain combining applied at the reception is analyzed. After theoretical derivation of the expression for the bit error rate (BER), the numerical integration with previously specified relative calculation error is performed. Numerical results are presented and confirmed by Monte Carlo simulations. The effects of the FSO link and receiver parameters on the BER performance are discussed. The results illustrate that the optimal APD gain in the minimum BER sense depends considerably on the link distance, atmospheric turbulence strength and receiver temperature. In addition, the value of this optimal gain is slightly different in the case of spatial diversity application compared with single channel reception.*

Keywords

Free space optical (FSO) communications, atmospheric turbulence, gamma-gamma distribution, error probability, avalanche photodiode (APD), on-off keying (OOK), equal gain combining (EGC).

1. Introduction

In contrast to the radio frequency networks, free space optical communications (FSO) can provide many advantages, which cause FSO to become increasingly popular and studied over the past decade. However, the atmospheric turbulence causes rapid intensity fluctuations at the received FSO signal, also known as fading or scintillation [1-3]. In order to describe the impact of atmospheric turbulence, many statistical models have been proposed. Good agreement between theoretical and experimental data in a wide range of turbulence conditions was the reason that the gamma-gamma distribution has been

accepted as the most suitable model [2-10]. Beside the atmospheric turbulence, system performances are degraded by the geometric loss and atmospheric attenuation caused by the absorption and scattering processes [2], [3].

Commercial FSO systems mostly deploy the intensity-modulation with direct detection (IM/DD) and the on-off keying (OOK), primarily because of the simplicity of its design and implementation [3]. The outage probability and channel capacity of FSO system with OOK over K-distributed channel was analyzed in [11].

At the FSO receiver with DD, the optical signal is first converted to an electrical one by a photodetector. All previously mentioned papers considered FSO systems with photodetectors using PIN photodiodes. The avalanche photodiodes (APDs) are widely used in optical receivers since they can provide larger values of responsivity [12]. The performance of APD receivers in FSO systems was considered in [13-15]. References [13], [14] are related to the subcarrier modulated FSO systems, while the pulse-position modulation (PPM) was considered in [15]. In [13], the BER of the rectangular quadrature amplitude modulation FSO system using the APD receiver over the log-normal and gamma-gamma channel was observed. The expressions for the BER and channel capacity of the FSO systems using the subcarrier binary phase-shift keying and APD photodiode were discussed in [14]. The BER performance of the binary PPM over lognormal FSO channel was analyzed in [15].

In order to improve system performances, spatial diversity techniques are often applied as a method for mitigation of irradiance fluctuations caused by atmospheric turbulence [16-19]. In [16], the BER performance of FSO transmission over strong atmospheric turbulence channel with spatial diversity was analyzed. The FSO system with subcarrier binary phase shift keying (BPSK) and spatial diversity over log-normal turbulent channel using PIN receiver has been observed in [17]. The BER analysis of BPSK subcarrier modulated FSO system with spatial diversity and PIN receiver was performed in [18], while weak to strong atmospheric channel is modeled by gamma-gamma distribution, and channel in saturation regime and beyond is modeled by negative exponential distribution.

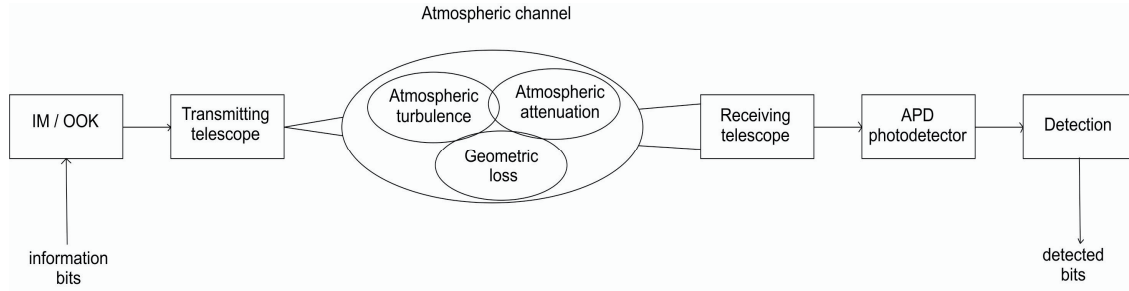


Fig. 1. Block diagram of the atmospheric turbulence FSO system using IM/OOK and APD receiver

In this paper, the IM/DD with OOK FSO system using APD receiver is observed. The atmospheric turbulence is modeled by very general gamma-gamma distribution. The impact of the receiver noise, including the APD shot noise and thermal noise, which are modeled as the additive white Gaussian noise, are taken into account. The BER expression for single-input and single-output (SISO) FSO channel is derived. In addition, the BER performance of the FSO system is observed when equal gain combining (EGC) diversity technique with two apertures is implemented at the reception. On the basis of the presented numerical results that are confirmed by Monte Carlo simulations, we discuss the BER dependence on the turbulence strength, APD gain, transmitted power, link distance and noise temperature. Numerical integration is controlled with given accuracy.

The rest of the paper is organized as follows. Section 2 describes the system model. In Section 3, the influence of the atmospheric turbulence, attenuation and geometric loss on BER performance is presented. In Section 4, BER expressions are derived and procedure for numerical integration is explained. Section 5 shows numerical and simulation results with discussions, while concluding remarks are given in Section 6.

2. System Model

The FSO system using IM/DD with OOK and APD receiver is shown in Fig. 1. At the transmitter, information bits are modulated by an electro-optical modulator IM/OOK whose output represents the intensity of the laser source. Next, the direction and the size of the laser beam are determined by the transmitting telescope which forwards the optical signal to the receiver over the atmospheric channel. At the receiver, the received laser beam is narrowed by telescope and passed to the APD photodetector, which is in charge of the optical to electrical signal conversion.

The instantaneous photocurrent at the input of the receiving APD photodetector, which corresponds to the information signal transmitted via laser beam, can be expressed as

$$r = axI = \begin{bmatrix} r_{on} \\ r_{off} \end{bmatrix} = \begin{bmatrix} a2P_tI \\ 0 \end{bmatrix}, \quad (1)$$

where a is the total link loss, and I is the normalized irradiance accounted for the intensity fluctuations due to atmospheric turbulence. The FSO system with OOK scheme is assumed, hence x represents the information „on“ or „off“ bit, i.e. x is either 0 or $2P_t$ where P_t is the average transmitted optical power.

After APD conversion, the electrical signal is

$$r_e = \begin{bmatrix} r_{e/on} \\ r_{e/off} \end{bmatrix} = \begin{bmatrix} gRr_{on} + n_{on} \\ gRr_{off} + n_{off} \end{bmatrix} = \begin{bmatrix} gRa2P_tI + n_{on} \\ 0 + n_{off} \end{bmatrix} \quad (2)$$

where g and R represent the average gain and responsivity of APD, respectively, and n is the total APD receiver noise different in „on“ and „off“ states (n_{on} and n_{off}). The total APD receiver noise is caused by shot noise, thermal noise and dark current. It is assumed that dark current is negligible, so n can be expressed as [13]

$$n = i_{Th} + i_{Sh} \quad (3)$$

where i_{Th} is the thermal noise and i_{Sh} is the APD shot noise. Thermal noise occurs due to the current fluctuation caused by the electrons thermal motion at any finite temperature, even in the absence of the signal transmission („off“ state). It does not depend on APD parts and can be modeled as the stationary Gaussian random process with the zero-mean value and variance [13]

$$\sigma_{Th}^2 = \sigma_{Th/on}^2 = \sigma_{Th/off}^2 = 4k_B \frac{T}{R_L} F_n \Delta f \quad (4)$$

where k_B denotes the Boltzmann constant, T is the receiver temperature in degree Kelvin, R_L denotes APD load resistance, F_n is the amplifier noise figure and Δf is the symbol effective noise bandwidth, here marked as $\Delta f = R_b/2$, where R_b is the bit rate.

Unlike thermal noise, the APD parts have effect on shot noise. The atmospheric turbulence causes the fluctuation in the received optical power and leads to uncertain in the shot noise variance. The shot noise can be modeled as the stationary zero-mean Gaussian random process with variance [13]

$$\sigma_{Sh}^2(I) = \begin{bmatrix} \sigma_{Sh/on}^2(I) \\ \sigma_{Sh/off}^2 \end{bmatrix} = \begin{bmatrix} 2qg^2 F_A RaI2P_t \Delta f \\ 0 \end{bmatrix} \quad (5)$$

where q is an electron charge and F_A denotes the excess noise factor of the APD given by

$$F_A = k_A g + (1 - k_A)(2 - 1/g) \quad (6)$$

where k_A is the ionization factor. The variance of the total APD noise can be expressed as

$$\sigma_n^2 = \begin{bmatrix} \sigma_{n/on}^2 \\ \sigma_{n/off}^2 \end{bmatrix} = \begin{bmatrix} \sigma_{Th}^2 + \sigma_{Sh/on}^2 \\ \sigma_{Th}^2 + \sigma_{Sh/off}^2 \end{bmatrix} = \begin{bmatrix} 4k_B \frac{T}{R_L} F_n \Delta f + 2qg^2 F_A RaI2P_t \Delta f \\ 4k_B \frac{T}{R_L} F_n \Delta f \end{bmatrix} \quad (7)$$

3. Channel Model

The optical signal transmission over the FSO channel is disrupted by atmospheric turbulence, attenuation and geometric loss.

The atmospheric turbulence is modeled by the gamma-gamma distribution given by [2], [3]

$$p_I(I) = \frac{2(\alpha\beta)^{(\alpha+\beta)/2}}{\Gamma(\alpha)\Gamma(\beta)} I^{(\alpha+\beta)/2-1} K_{\alpha-\beta}(2\sqrt{\alpha\beta}I) \quad (8)$$

where $\Gamma(\cdot)$ is the gamma function [20, eq. (8.310.1)] and $K_\nu(\cdot)$ is the ν^{th} -order modified Bessel function of the second kind [20, eq. (8.432)]. The parameters α and β represent the effective numbers of small-scale and large scale cells, respectively, and can be related to the atmospheric conditions. If the plane wave propagation and zero inner scale is assumed, the parameters α and β can be expressed as [2], [3]

$$\alpha = \left(\exp \left[\frac{0.49\sigma_R^2}{(1 + 1.11\sigma_R^{12/5})^{7/6}} \right] - 1 \right)^{-1}, \quad (9)$$

$$\beta = \left(\exp \left[\frac{0.51\sigma_R^2}{(1 + 0.69\sigma_R^{12/5})^{5/6}} \right] - 1 \right)^{-1},$$

where σ_R^2 is the Rytov variance and is used as a metric of the strength of turbulence. It is given by

$$\sigma_R^2 = 1.23C_n^2 k^{7/6} L^{11/6} \quad (10)$$

where $k = 2\pi/\lambda$ is the wave-number, λ is the wavelength, L is the propagation distance, and C_n^2 is the refractive index structure parameter, which typically varies from 10^{-17} to $10^{-13} \text{ m}^{-2/3}$ as turbulence strength varies from weak to strong conditions. To simplify, σ_R is used as a metric of turbulence strength which is combination of distance, wavelength and the parameter C_n^2 .

The atmospheric attenuation and geometric loss are described by total link loss given by [13], [14]

$$a = \frac{A}{\pi \left(\frac{\theta L}{2} \right)^2} e^{-\beta_v L} \quad (11)$$

where β_v denotes the extinction coefficient, L is the link distance, θ is the angle of divergence in radians and A is the detector area at receiver equals to $A = \pi D^2/4$, where D represents the diameter of the receiver's aperture.

4. BER Analysis

In this section, analytical BER expression for single FSO channel is derived. Next, EGC diversity technique is implemented at the receiver in order to improve BER performance.

4.1 SISO Channel

The conditional BER of FSO using IM/DD with OOK is determined as

$$P_{e/I} = P(on)P(off|on) + P(off)P(on|off) \quad (12)$$

where $P(on)$ and $P(off)$ represent the probabilities of transmitting „on“ and „off“ bits, respectively, $P(off|on)$ is the probability of detecting „off“ bit when „on“ bit is sent and $P(on|off)$ is otherwise. The previous BER is conditional on the received optical signal that is random process whose probability density function is given by (8). It is considered that $P(on) = P(off) = 0.5$, so the conditional BER can be found as

$$P_{e/I} = \frac{1}{2} [P(off|on) + P(on|off)]. \quad (13)$$

The noise variances in „on“ and „off“ states are different, and denoted by $\sigma_{n/on}^2$ and $\sigma_{n/off}^2$, respectively. On the basis of the analysis presented in [12, p. 163], the probabilities $P(off|on)$ and $P(on|off)$ are given by

$$P(off|on) = \frac{1}{2} \operatorname{erfc} \left(\frac{d_{on} - d_{th}}{\sqrt{2\sigma_{n/on}^2}} \right), \quad (14)$$

$$P(on|off) = \frac{1}{2} \operatorname{erfc} \left(\frac{d_{th} - d_{off}}{\sqrt{2\sigma_{n/off}^2}} \right) \quad (15)$$

where $\operatorname{erfc}(\cdot)$ is the complementary error function [20, eq. (8.250.4)], $d_{on} = gRa2P_t$ is the electrical „on“ signal and $d_{off} = 0$ is the electrical „off“ signal generated at the receiver and d_{th} is the decision threshold. Now, (13) is

$$P_{e/I} = \frac{1}{4} \left[\operatorname{erfc} \left(\frac{d_{on} - d_{th}}{\sqrt{2\sigma_{n/on}^2}} \right) + \operatorname{erfc} \left(\frac{d_{th} - d_{off}}{\sqrt{2\sigma_{n/off}^2}} \right) \right]. \quad (16)$$

The simplicity in design and implementation are the main reason for employing OOK in commercial FSO systems. However, it is needed to set a decision threshold, which is a major problem in this system realization.

From (16), it can be noted that the BER depends on d_{th} . The decision threshold can be optimized under condition that $P(on|off) = P(off|on)$ [12, p. 164]:

$$d_{th} = \frac{\sigma_{n/off}d_{on} + \sigma_{n/on}d_{off}}{\sigma_{n/off} + \sigma_{n/on}}. \quad (17)$$

This choice of decision threshold leads to the conditional BER for the considered system in the form of

$$P_{e/I} = \frac{1}{2} \operatorname{erfc}\left(\frac{Q(I)}{\sqrt{2}}\right) \quad (18)$$

where the parameter $Q(I)$ is given by [12, p. 164]

$$Q(I) = \frac{d_{on} - d_{off}}{\sigma_{n/on} + \sigma_{n/off}} = \frac{gRa2P_I}{\sigma_{n/on} + \sigma_{n/off}}. \quad (19)$$

The average BER over gamma-gamma fading channel is obtained by averaging (18) over the received optical irradiance:

$$P_e = \frac{1}{2} \int_0^\infty \operatorname{erfc}\left(\frac{gRa2P_I}{\sqrt{2}(\sigma_{n/on} + \sigma_{n/off})}\right) p_I(I) dI. \quad (20)$$

By substituting (7) and (8) into (20), equation (21) on the top of the next page is obtained. Numerical values of the BER are obtained by using Gaussian quadrature rule [21, eq. (25.4.45), p. 923],

$$P_e \cong \sum_{i=1}^M w_i f(x_i), \quad (22)$$

where $f(x) = \operatorname{erfc}\left(\frac{gRa2P_I x}{\sqrt{2\sigma_{Th}^2} \left(1 + \sqrt{1 + 2qg^2 F_A Rax2P_I \Delta f}\right)}\right).$ (23)

Abscissas x_i and weights w_i are obtained from the moments of the weight function $p_I(I)$. It is easily shown that the moments are [20, eq. (6.561.16)]:

$$m_k = \frac{\Gamma(\alpha + k)\Gamma(\beta + k)}{\Gamma(\alpha)\Gamma(\beta)(\alpha\beta)^k}. \quad (24)$$

With moments expressed in closed form, one can then proceed with Chebyshev's algorithm in order to obtain the required abscissas and weights for the quadrature rule [22].

Since there is a question of the order of the quadrature rule used, which is reflected by parameter M in (22), we need to estimate a reasonable value of M for the calculations. Therefore, we have conducted a numerical experiment and the results are presented in Fig. 2. In general, we see that the relative error of calculated BER decreases as the number of points used increases. Another observation can be made, that the required number of points to reach a certain precision differs significantly as the receiver is placed further from the transmitter. In particular, in the case of the optical radiated power of 0 dBm, we have concluded that for the 1% relative error, the required number of points is about 65 when the receiver is located 1000 m from the transmitter, and the required number of points drops to about 6 when the receiver is 3000 m away from the transmitter.

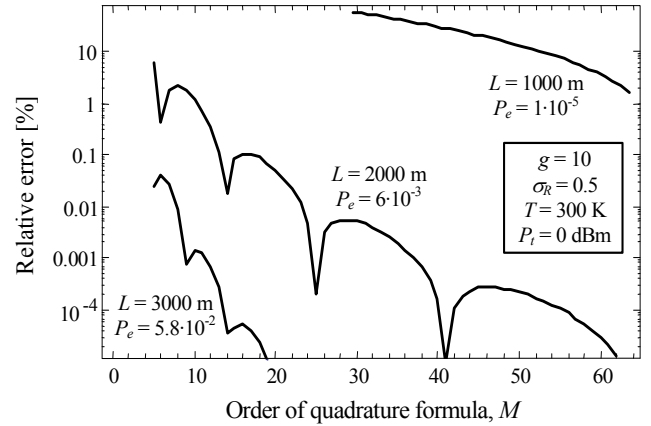


Fig. 2. Relative error of calculated BER, versus the order of the quadrature rule used.

4.2. EGC Diversity Technique

When EGC diversity technique with two apertures is implemented at the reception, photocurrents from each aperture are summed coherently with equal weights of unity.

At the reception, the beam footprint has to cover the whole field of view of both detectors, so each detector area is two times smaller than the case when there is no diversity [16-19]. Hence, the atmospheric attenuation is two times smaller compared to the attenuation when diversity is not applied:

$$a_{EGC} = \frac{A_{EGC}}{\pi\left(\frac{\theta L}{2}\right)^2} e^{-\beta L} = \frac{a}{2} \quad (25)$$

where A_{EGC} is the detector area at receiver when diversity with two apertures is applied.

When this kind of system is considered, the average BER expression can be obtained by averaging (18) over irradiance at the EGC output I_{EGC} :

$$P_e = \frac{1}{2} \int_0^\infty \operatorname{erfc}\left(\frac{gRa_{EGC} 2P_I I_{EGC}}{\sqrt{2}(\sigma_{EGC/on} + \sigma_{EGC/off})}\right) \times p_{I_{EGC}}(I_{EGC}) dI_{EGC}, \quad (26)$$

where $p_{I_{EGC}}(I)$ is the PDF of EGC output and $\sigma_{EGC/on}$ and $\sigma_{EGC/off}$ are the variances of the total APD noise in „on“ and „off“ states of the observed system, respectively.

The variances of the total APD noise represent the sum of total variances of first and second aperture:

$$\sigma_{EGC}^2 = \begin{bmatrix} \sigma_{EGC/on}^2 \\ \sigma_{EGC/off}^2 \end{bmatrix} = \begin{bmatrix} \sigma_{I_1/on}^2 + \sigma_{I_2/on}^2 \\ \sigma_{I_1/off}^2 + \sigma_{I_2/off}^2 \end{bmatrix}. \quad (27)$$

As it was mentioned, thermal noise does not depend on APD parts, so it will be equal at both apertures. Otherwise, APD parts and intensity fluctuation effect on shot noise, so there will be difference in shot variances of first

$$P_e = \frac{(\alpha\beta)^{(\alpha+\beta)/2}}{\Gamma(\alpha)\Gamma(\beta)} \int_0^\infty I^{(\alpha+\beta)/2-1} K_{\alpha-\beta}(2\sqrt{\alpha\beta}I) \operatorname{erfc} \left(\frac{gRa2P_t I}{\sqrt{2} \left(\sqrt{4k_B \frac{T}{R_L} F_n \Delta f} + 2qg^2 F_A Ra I 2P_t \Delta f + \sqrt{4k_B \frac{T}{R_L} F_n \Delta f} \right)} \right) dI. \quad (21)$$

and second aperture. Since $I_{EGC} = I_1 + I_2$, following (7), the variances of the total APD noise in „on“ and „off“ states are found as:

$$\sigma_{EGC}^2 = \begin{bmatrix} \sigma_{EGC/on}^2 \\ \sigma_{EGC/off}^2 \end{bmatrix} = \begin{bmatrix} 2 \cdot 4k_B \frac{T}{R_L} F_n \Delta f + 2qg^2 F_A Ra_{EGC} I_{EGC} 2P_t \Delta f \\ 2 \cdot 4k_B \frac{T}{R_L} F_n \Delta f \end{bmatrix} \quad (28)$$

When EGC with two apertures is applied, $p_{I_{EGC}}(I)$ is the joint PDF of the vector $\mathbf{I} = (I_1, I_2)$ [16]. It is assumed that irradiances of both apertures experience independent identical distributions (i.i.d.), so their PDFs will be the same ($p_{I_1}(I) = p_{I_2}(I) = p_I(I)$) as in (8). So, the PDF of EGC output can be found as:

$$p_{I_{EGC}}(I) = \int_0^I p_I(I - I_2) p_I(I_2) dI_2. \quad (29)$$

The average BER expression of FSO system with two i.i.d. apertures can be found by substituting (28) and (29) into (26).

5. Numerical Results

In this section, the numerical results, obtained by derived equations (21) and (26), are presented and discussed. Also, numerical results are confirmed by Monte Carlo simulations. The values of the system parameters that are necessary for calculations are given in Tab. 1. These values are similar to those exploited in [13], [14].

Fig. 3 shows the BER dependence on the average APD gain for the various propagation distances of FSO system with and without EGC. The system has better performance when EGC is implemented at the receiver. It is noted that the performance can be optimized by a proper selection of the average APD gain because the minimum of BER curve exists. The value of optimal APD gain g in the minimum BER sense depends on the link distance L . This optimal g value increases with increasing the link distance L . For example, in the SISO case, the optimal g increases from $g = 35.1$ to $g = 39.02$ with the FSO link distance increasing from $L = 1500$ m to $L = 3500$ m. Also, optimal g is increased when EGC is implemented at the reception. When FSO link distance is $L = 2500$ m, the optimal APD gain is $g = 37.1$ for SISO channel, and $g = 39.1$ when EGC with two apertures is applied.

name	symbol	value
Optical wavelength	λ	1.55 μm
Boltzmann constant	k_B	1.38×10^{-23} W/kHz
Electron charge	q	1.6×10^{-19} C
APD load resistance	R_L	1000 Ω
Amplifier noise figure	F_n	2
Bit rate	R_b	2 Gb/s
Ionization factor	k_A	0.7 (InGaAs APD)
Responsivity	R	1 A/W
Receiver's aperture diameter	D	0.02 m
Angle of divergence	θ	10^{-3} rad
Extinction coefficient	β_v	0.1 dB/km

Tab. 1. Constants and system parameters.

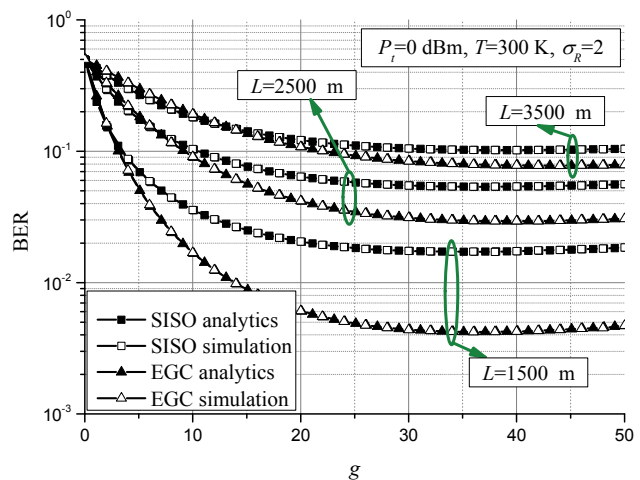


Fig. 3. BER dependence on average APD gain for different values of FSO link distance.

The effect of the receiver noise temperature T on the optimal average APD gain is illustrated in Fig. 4. With varying the temperature T , the optimal gain is changing. When no diversity is applied, as the temperature increases from $T = 100$ K to $T = 500$ K, the optimal gain increases from $g = 21.08$ to $g = 32.03$. Implementation of EGC at the reception leads to slight increasing of optimal APD gain. In addition, when the average APD gain reaches higher values (exceeds 60), the effect of the receiver noise temperature on BER performance becomes less expressed. As expected, the numerical results illustrate that the system has lower values of BER at lower temperatures T .

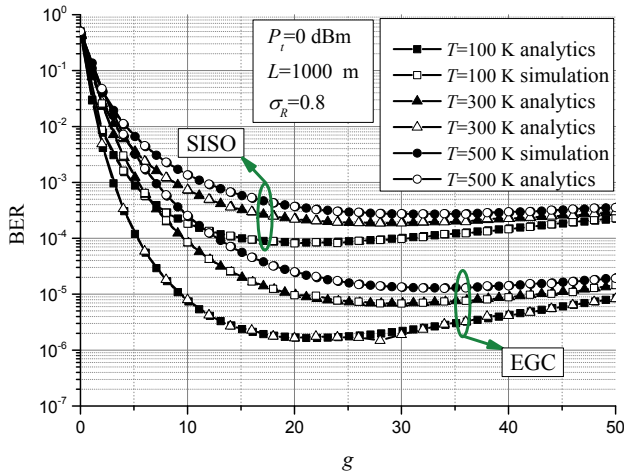


Fig. 4. BER dependence on the average APD gain for different values of receiver noise temperature T .

In Fig. 5, the BER dependences on g for different values of turbulence strength σ_R is presented. The improvement of BER performance is noticed with implementation of EGC diversity. The system has better performance for lower values of turbulence strength, so with increasing the parameter σ_R , the turbulence conditions are more expressed. The influence of the average APD gain is less expressed in strong turbulence conditions.

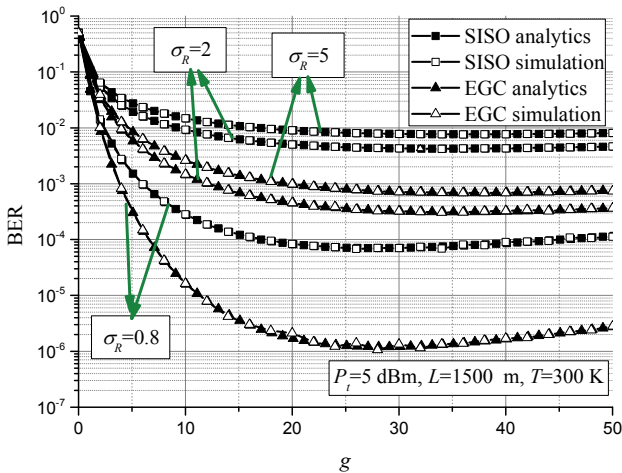


Fig. 5. BER dependence on the average APD gain for different values of turbulence strength.

The BER dependences on the average transmitted power for different values of propagation path length are presented in Fig. 6 in the cases of SISO and EGC systems. As expected, the BER values increase with transmitted power decreasing and link distance increasing. In the case of SISO channel, in order to achieve the BER of 10^{-2} , if the link distance increases from $L = 1500$ m to $L = 3500$ m, the power penalty that should be paid is about 7.59 dBm. When $L = 1500$ m and target value of BER is 10^{-3} , applying EGC with two apertures at the reception leads to saving in average transmitted power of 10.1 dBm, but the system complexity is greater.

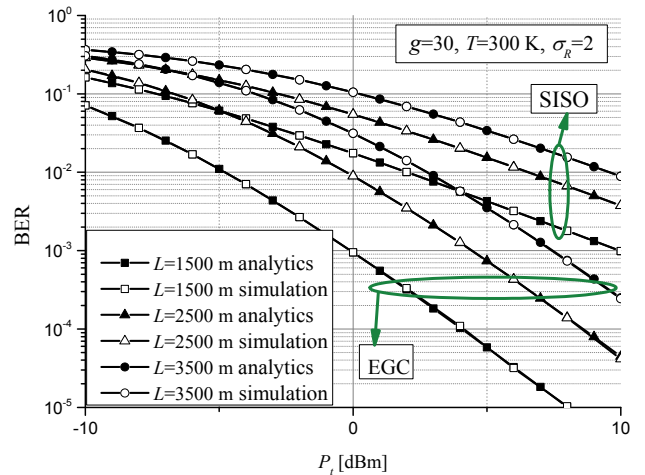


Fig. 6. BER dependence on average transmitted power for different values of FSO link distance.

In Fig. 7, the BER dependences on the average transmitted power for different values of the receiver noise temperature is observed. With increasing the temperature, there is a higher value of the BER for the same transmitted power. When $T = 300$ K and available average transmitted power is $P_t = -5$ dBm, BER value is 4×10^{-3} and 6.5×10^{-5} for SISO and EGC system, respectively. Hence, improvement of system performance is noticed with applying EGC at the reception.

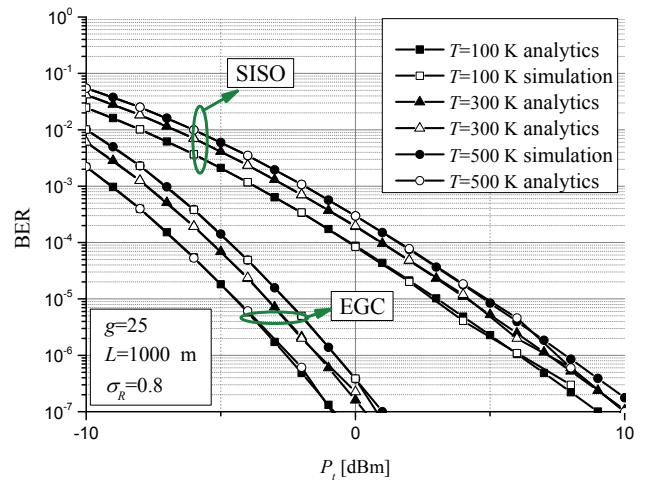


Fig. 7. BER dependence on average transmitted power for different values of receiver noise temperature.

The BER performances in different atmospheric conditions for SISO and EGC systems are shown in Fig. 8. To achieve a certain value of BER, the greater transmitted power P_t is needed when σ_R is higher, i.e. in strong turbulence conditions. For SISO system, when average transmitted power is 0 dBm, for weak and strong turbulence conditions (corresponding to the values of $\sigma_R = 0.8$ and $\sigma_R = 5$), the BER values are 1.8×10^{-3} and 2.4×10^{-2} , respectively. When the target value of BER is 10^{-3} , in moderate turbulence conditions, i.e. $\sigma_R = 2$, there is a saving in optical transmitted power of 10 dBm with implementation of EGC receiver with two apertures.

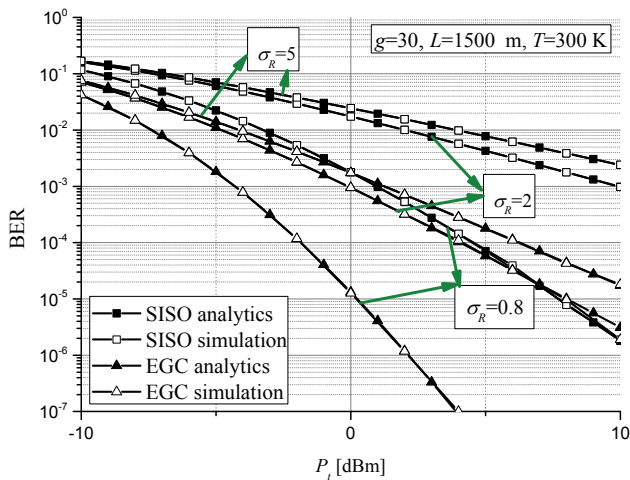


Fig. 8. BER dependence on average transmitted power for different values of turbulence strength.

6. Conclusion

In this paper, the BER performance of FSO system using IM/DD with OOK and APD receiver has been observed. The efficient numerical method for BER calculation for the wide range of the values of the channel and receiver parameters has been presented. Also, system is improved by implementing EGC technique with two apertures at the reception. The numerical results are confirmed by Monte Carlo simulations. The results have illustrated that optimal APD gain in the minimum BER sense is considerably influenced by FSO link distance, receiver temperature and turbulence conditions. This optimal gain increases with increasing distance, temperature and Rytov parameter. The results have shown that the proper choice of optimal APD gain is especially important in the more severe atmospheric turbulence, as well as in the case of small distances and low temperature values. The results illustrated that when the average APD gain reaches higher values, the effect of the receiver noise temperature on BER performance becomes less expressed. The effect of temperature on BER is pronounced in the range around optimal APD gain. The observed system performance can be significantly improved with proper selection of the optimal APD gain. In addition, the results illustrated that BER performance can be significantly improved by implementation of dual branch EGC technique. According to the presented results the diversity gains of about 10 dBm can be achieved in the observed system.

Acknowledgements

This paper was supported in part by the Ministry of Science of Republic of Serbia under grants TR-32028 and III-44006 and in part by the Norwegian Ministry of Foreign Affairs under the project NORBAS (grant 2011/1383) headed by NTNU. The authors also acknowledge the ICT

COST Action IC1101. The authors should like to thank the anonymous reviewers whose suggestions and comments improved the quality of the paper.

References

- [1] HENNIGER, H., WILFERT, O. An introduction to free-space optical communications. *Radioengineering*, 2010, vol. 19, no. 2, p. 203 - 212.
- [2] ANDREWS, L. C., PHILIPS, R. N. *Laser Beam Propagation through Random Media*. 2nd ed. Bellingham (USA): Spie Press, 2005.
- [3] GHASSEMLOOY, Z., POPOOLA, W., RAJBHANDARI, S. *Optical Wireless Communications: System and Channel Modelling with MATLAB*. Boca Raton (USA): CRC Press, 2013.
- [4] AL-HABASH, M. A., ANDREWS, L. C., PHILIPS, R. L. Mathematical model for the irradiance probability density function of a laser beam propagating through turbulent media. *Optical Engineering*, 2001, vol. 40, no. 8, p. 1554 - 1562.
- [5] TSIFTSIS, T. A. Performance of heterodyne wireless optical communication systems over gamma-gamma atmospheric turbulence channels. *Electronic Letters*, 2008, vol. 44, no. 5, p. 372 - 373.
- [6] ANGUITA, J. A., DJORDJEVIC, I. B., NEIFEILD, M. A., VASIC, B. V. Shannon capacities and error-correction codes for optical atmospheric turbulent channels. *Journal of Optical Networking*, 2005, vol. 4, no. 9, p. 586 - 601.
- [7] FARID, A. A., HRANILOVIC, S. Outage capacity optimization for free space optical links with pointing errors. *IEEE/OSA Journal of Lightwave Technology*, 2007, vol. 25, no. 7, p. 1702 - 1710.
- [8] GAPPMAIR, W., HRANILOVIC, S., LEITGEB, E. Performance of PPM on terrestrial FSO links with turbulence and pointing errors. *IEEE Communications Letters*, 2005, vol. 14, no. 5, p. 468 - 470.
- [9] PROKEŠ, A. Modeling of atmospheric turbulence effect on terrestrial FSO link. *Radioengineering*, 2009, vol. 18, no. 1, p. 42 - 47.
- [10] GAPPMAIR, W., HRANILOVIC, S., LEITGEB, E. OOK performance for terrestrial FSO links in turbulent atmosphere with pointing errors modelled by Hoyt distributions. *IEEE Communications Letters*, 2011, vol. 15, no. 8, p. 875 - 877.
- [11] SANDALIDIS, H. G., TSIFTSIS, T. A. Outage probability and ergodic capacity of free-space optical links over strong turbulence. *Electronic Letters*, 2008, vol. 44, no. 1, p. 46 - 47.
- [12] AGRAWAL, G. P. *Fiber-Optic Communications Systems*. 3rd ed. New York: John Wiley & Sons, 2002.
- [13] VU, B. T., DANG, N. T., TRUONG, C.-T., PHAM, A. T. Bit error rate analysis of rectangular QAM/FSO systems using an APD receiver over atmospheric turbulence channels. *IEEE/OSA Journal of Optical Communications and Networking*, 2013, vol. 5, no. 5, p. 437 - 446.
- [14] LUONG, D. A., TRUONG, C.-T., PHAM, A. T. Effect of avalanche photodiode and thermal noises on the performance of binary phase-shift keying-subcarrier-intensity modulation/free-space optical systems over turbulence channels. *IET Communications*, 2013, vol. 7, no. 8, p. 738 - 744.
- [15] KIASALEH, K. Performance of APD-based, PPM free-space optical communication systems in atmospheric turbulence. *IEEE Transactions on Communications*, 2005, vol. 53, no. 9, p. 1455 - 1461.

- [16] TSIFTISIS, T. A., SANDALIDIS, H. G., KARAGIANNIDIS, G. K., UYSAL, M. Optical wireless links with spatial diversity over strong atmospheric turbulence channels. *IEEE Transactions on Wireless Communications*, 2009, vol. 8, no. 2, p. 951 - 957.
- [17] POPOOLA, W. O., GHASSEMLOOY, Z., ALLEN, J. I. H., LEITGEB, E., GAO, S. Free-space optical communication employing subcarrier modulation and spatial diversity in atmospheric turbulence channel. *IET Optoelectronics*, 2008, vol. 2, no. 1, p. 16 - 23.
- [18] POPOOLA, W. O., GHASSEMLOOY, Z. BPSK subcarrier intensity modulated free-space optical communications in atmospheric turbulence. *IEEE/OSA Journal of Lightwave Technology*, 2009., vol. 27, no. 8, p. 967-973.
- [19] NTOGARI, G., KAMALAKIS, T., SPHICOPOULOS, T. Analysis of indoor multiple-input multiple-output coherent optical wireless systems. *IEEE/OSA Journal of Lightwave Technology*, 2012, vol. 30, no. 3, p. 317 - 324.
- [20] GRADSHTEYN, I. S., RYZHIK, I. M. *Table of Integrals, Series, and Products*. 6th ed. New York: Academic, 2000.
- [21] ABRAMOWITZ, M., STEGUN, I. *Handbook of Mathematical Functions*. New York: Dover Publications, 1972.
- [22] MILOVANOVIC, G. V. *Numerical Analysis Part 2*. Belgrade: Naučna knjiga, 1991. (in Serbian).

About Authors ...

Milica I. PETKOVIĆ was born in Knjazevac, Serbia, in 1986. She received the M.Sc. degree in Electrical Engineering from the Faculty of Electronic Engineering, University of Nis, Serbia, in 2010, and enrolled Ph.D studies at same faculty. Her research interests include communication

theory, wireless and optical communication systems, application of different modulation techniques and modeling of fading channels.

Goran T. ĐORĐEVIĆ was born in Nis, Serbia. He received his Dipl. Ing., M.S., and PhD degrees in Electrical Engineering from the Faculty of Electronic Engineering, University of Nis, Serbia, in 1996, 1999 and 2005, respectively. His area of interest is communication theory and applications in satellite, wireless and free space optical communication systems. His current research interests include application of different modulation formats and error control codes in free space optics and satellite fixed and mobile services, as well as modeling and simulation of fading channels. He authored more than 20 journal and 100 conference publications. Currently he is an Associate Professor at the Department of Telecommunications, Faculty of Electronic Engineering, University of Nis, Serbia. He teaches courses of Communication Theory, Information Theory, Modeling and Simulation of Communication Systems and Satellite Communications.

Dejan N. MILIĆ was born in Nis, Serbia in 1972. He received B.S., M.S., and Ph.D. degrees in Electrical Engineering from the Faculty of Electronic Engineering, University of Nis, Serbia, in 1997, 2001 and 2005, respectively. He is currently an Associate Professor at the Department of Telecommunications at the same Faculty, and there he teaches optical communications and coherent communication systems. Other areas of research include communication theory, modulation and wireless communications.